Acta Biochimica Polonica

Vol. 51 No. 1/2004

153–160

QUARTERLY

Communication

Effect of antisense peptide binding on the dimerization of human cystatin C — gel electrophoresis and molecular modeling studies★✪

Krystyna Stachowiak[1]✉, Sylwia Rodziewicz-Motowidło[1], Renata Sosnowska[1], Franciszek Kasprzykowski[1], Leszek Łankiewicz[1], Anders Grubb[2] and Zbigniew Grzonka[1]

[1]*Faculty of Chemistry, University of Gdańsk, Gdańsk, Poland;* [2]*Department of Clinical Chemistry, University Hospital, Lund, Sweden*

Received: 31 October, 2003; revised: 02 March, 2004; accepted: 09 March, 2004

Key words: human cystatin C, antisense peptides, dimerization, molecular dynamics

Human cystatin C (HCC) shows a tendency to dimerize. This process is particularly easy in the case of the L68Q HCC mutant and might lead to formation of amyloid deposits in brain arteries of young adults. Our purpose was to find ligands of monomeric HCC that can prevent its dimerization. Eleven antisense peptide ligands of monomeric HCC were designed and synthesized. The influence of these ligands on HCC dimerization was studied using gel electrophoresis and molecular modeling methods. The results suggest that all the designed peptides interact with monomeric HCC facilitating its dimerization rather than preventing it.

Cystatins are natural, single-chain proteins that reversibly inhibit cysteine proteases. Three types of cystatins occur in higher organisms. Type 1, also called stefins, includes

★Presented at the 17th Polish Peptide Symposium, August 31st–September 4th, 2003, Łódź, Poland.

✪This work was supported by the State Committee for Scientific Research (KBN, Poland, 0298/P04/2001/21) and University of Gdańsk (grant BW/8000-5-0243-3) and the Swedish Scientific Council (project 5196).

✉Corresponding author: K. Stachowiak, Faculty of Chemistry, University of Gdańsk, 80-952 Gdańsk, J. Sobieskiego 18, Poland; tel. (48 58) 345 0367; fax. (48 58) 341 0357; e-mail: krysias@chemik.chem.univ.gda.pl

Abbreviations: DCM, dichloromethane; DIPCDI, 1,3-diisopropylcarbodiimide; DMF, dimethylformamide; Fmoc, 9-fluorenylmethoxycarbonyl; HCC, human cystatin C; HOBt, 1-hydroxybenzotriazole; NMP, *N*-methyl-2-pyrrolidinone; Pbf, 2,2,4,6,7-pentamethyl-dihydrobenzofuran-5-sulfonyl, PBS, phosphate-buffered saline; TFA, trifluoroacetic acid; Trt, trityl.

intracellular cystatin A and B. Type 2 cystatins comprise extracellular and/or transcellular cystatins C, D, E, F, S, SN and SA. Type 3 cystatins, named kininogens, act in the intravascular environment. Human cystatin C (HCC) is present in all extracellular fluids where it inhibits endogenous cysteine proteases – for example, cathepsins B, H, K, L and S (Grubb, 2000; Grzonka *et al.*, 2001). HCC is 120 amino-acid residues long and contains four Cys residues, which form two characteristic disulfide bridges. The known 3D-structures of cystatins (chicken cystatin (Bode *et al.*, 1988; Dieckmann *et al.*, 1993; Engh *et al.*, 1993), cystatin B in complex with papain (Stubbs *et al.*, 1990), cystatin A (Martin *et al.*, 1995; Staniforth *et al.*, 2001), HCC in dimeric form (Janowski *et al.*, 2001)) have revealed similar overall protein fold, with three regions implicated in interactions with the enzyme. Structurally, each cystatin monomer consists of a core with a five-stranded antiparallel β-sheet wrapped around a central helix (PDB entry: 1CEW). Two hairpin loops (L1 and L2), together with the N-terminal fragment are involved in interactions with target proteolytic enzymes (Grzonka *et al.*, 2001). HCC is monomeric in its native physiological state while in pathological conditions it is present as an extracellular dimer. In pathological processes HCC and its L68Q mutant constitute a major part of amyloid deposits in brain arteries of young adults, which leads to brain haemorrhages and finally death in patients with hereditary cystatin C amyloid angiopathy (HCCAA) (Ghiso *et al.*, 1986; Jensson *et al.*, 1987; Abrahamson, 1996; Olafsson & Grubb, 2000). The HCCAA occurs endemically in the population of Iceland (Olafsson & Grubb, 2000). The L68Q HCC mutant has a proteinase inhibitory activity similar to that of the wild type protein and probably a 3D structure very similar to that of the wild type (Ekiel *et al.*, 1997; Gerhatz *et al.*, 1998). However, the L68Q variant of HCC forms dimers in human body fluids more easily than the wild type. The dimerization of the L68Q variant progresses to a significant extent at normal body temperature, as does a coupled aggregation process leading to successive formation of large insoluble cystatin aggregates. The formation of wild type HCC dimers is favoured by elevated but pre-denaturating temperatures or levels of denaturant (Ekiel & Abrahamson, 1996; Jerela & Zerovnik 1999). It has been proposed that the HCC dimer (PDB entry: 1G96) is formed by the exchange of three-dimensional 'β-sheet subdomains' between the two subunits (Janowski *et al.*, 2001). The process in which a domain in a protein breaks its noncovalent bonds with the remainder of the molecule and is replaced by the corresponding domain of a second identical protein molecule is named 3D domain swapping (JaskÓlski, 2001).

The aim of the present investigation was to design inhibitors of HCC dimerization. Until now, no inhibitor of this process is known. These molecules could be potential drugs in the treatment of human cystatin C amyloid angiopathy. We synthesized eleven potential peptide ligands of monomeric HCC and investigated their influence on the dimerization process. The stability of the HCC complexes with the ligands was also determined by molecular modeling methods. The amino-acid sequences of the ligands were designed upon antisense nucleotide sequence of these HCC fragments which are, according to a proposed pathway (Janowski *et al.*, 2001), directly involved in the early stage of the dimerization process. By definition, the coding strand of DNA is called sense chain and generates sense peptides or proteins. The complementary, non-coding strand of DNA is called antisense DNA chain. The peptides whose amino-acid sequences are derived from the nucleotide sequence (5'→3' reading) of the complementary, antisense, strand of DNA (or more strictly from codons of a complementary mRNA) are called antisense peptides. It has been found that antisense peptides are able to interact with sense peptides and pro-

teins with significant selectivity and moderate affinity (Mekler, 1969; Blalock, 1995; Baranyi *et al.*, 1995; Heal *et al.*, 2002). In terms of the Blalock (1990; 1995) molecular recognition theory "inverse forces" act within mutually complementary peptides because of their opposite profiles of hydropathy (measured on the Kyte-Doolittle hydropathy scale of amino acids (Kyte & Doolittle, 1982)). As a result, sense and antisense peptides have complementary shapes which enable their interaction. The antisense-sense phenomenon has been successfully applied for purification of peptides by affinity chromatography (Zhao *et al.*, 2001), for identifications of unknown receptors (Blalock, 1999; Heal *et al.*, 2002), and also in designing new inhibitors of enzymes (Heal *et al.*, 1999; Sautebin *et al.*, 2000). Moreover, the antisense sequence of HCC loop L1 was found in β chain of human C4 protein (Ghiso *et al.*, 1990) and specific interactions between these two segments of native proteins were shown. We assumed that our antisense peptides would bind to the complementary fragments of HCC and that this binding might stabilize the monomeric form of the protein.

MATERIALS AND METHODS

Materials. Fmoc-amino acids were purchased from Bachem AG. The TentaGel R Ram was obtained from RAPP Polymere (Germany). HCC, obtained by *Escherichia coli* expression, was produced and purified as previously described (Abrahamson *et al.*, 1988).

Peptide synthesis. All peptide ligands were synthesized by the solid-phase method using Fmoc chemistry. TentaGel R Ram (substitution of Fmoc groups 0.17 meq/g) was used as support. The syntheses were carried out on an automatic synthesizer (Milli-Gen 9050 Plus, model A). During the synthesis the following amino-acid derivatives were used: Fmoc-Ala, Fmoc-Gly, Fmoc-Leu, Fmoc-Met, Fmoc-Val, Fmoc-Phe, Fmoc-Pro, Fmoc-Ser(OBu^t), Fmoc-Asp(OBu^t), Fmoc-Asn(Trt), Fmoc-Glu(OBu^t), Fmoc-Gln(Trt), Fmoc-Arg(Pbf), Fmoc-His(Trt), Fmoc-Tyr(OBu^t), Fmoc-Thr(OBu^t). Deblockings were performed with 20% piperidine in DMF/NMP (1:1) with addition of 1% Triton X-100. Couplings were achieved using DIPCDI/HOBt in the mixture DMF/NMP/DCM (1:1:1) with addition of 1% Triton X-100, for 60 min. After the syntheses had been completed, the peptides were removed from the resin together with the side chain deprotections in a one-step procedure by acidolysis, using TFA/phenol/triisopropylsilane/H_2O (88:5:2:5, by vol.). Purification was carried out on a semi-preparative reversed-phase C-8 HPLC column (Kromasil Kr 100-5-C-8, 10×250mm) with solvent A (0.1% TFA in water) and solvent B (0.08% TFA in 80% aqueous solution of acetonitrile) and detection wavelength λ = 230 nm. The purity of the peptides was > 96%. All the peptides showed correct molecular mass as measured by MALDI-TOF mass spectroscopy (VG Mass Lab).

HCC dimerization. The study of HCC dimer formation was performed by incubating the synthesized peptides in a solution of 1 mg/ml of HCC for 7 days at 37°C. The solution was 0.05 M sodium phosphate buffer, pH 7.4, containing 0.1 M sodium chloride and 0.5 M guanidine hydrochloride. We followed the progress of HCC dimerization using agarose gel electrophoresis according to the procedure described by Jeppsson *et al.*, (1979). We used 1% analytical agarose gel in 0.078 M barbital buffer, pH 8.6. The HCC dimers were previously shown to have a more anodal mobility than monomeric HCC (Grubb, 2000).

Construction of the 'closed' HCC monomer model. The experimental three-dimensional structure of monomer-HCC is unknown. Therefore we built a monomer model of HCC on basis of the known X-ray structure of HCC dimer (PDB entry: 1G96) and the 3D structure of chicken monomer cystatin C. The monomer-HCC model was built as follows. The bonds N-αC in two A^{58} (in dimer) were

cut, and next the N atom of A^{58} of one cystatin C molecule was joined with the αC atom of A^{58} of the other cystatin C molecule. This construction corresponds to the monomeric-mimicking units of dimeric cystatin C. This procedure was made with the SYBYL6.8 program (SYBYL ver. 6.6 © 2000). The X-ray structure of HCC dimer does not contain the N-terminal fragment (first 8 amino-acid residues) of cystatin C, because of its flexibility. Therefore our monomer model of HCC has 112 amino-acid residues, too. The constructed structure of the HCC monomer was adapted to further calculations by energy minimization.

Theoretical calculations. All simulations were carried out using the AMBER 7.0 program (Case *et al.*, 1997), and the AMBER all-atom force field. The details of the procedure are in Table 1. The crude systems were initially minimized *in vacuo* to remove close van der Waals contacts. This (and next minimization) consisted of 10 000 steps. Before surrounding the complex (HCC–ligand) with water molecules, Na^+ and Cl^- charge-balancing counterions were added in positions with favourable ion–residue interactions to neutralize charges on the protein–ligand surface. The AMBER CION program was used, which adds counterions in a shell around a molecule using a Coulombic potential on a grid. Next, all structures were optimized by energy minimization in water box. Constraints between the ligand and the protein were added during the minimizations and further molecular dynamics (MD). The positions of backbone atoms of HCC during these minimization and next MD were not changed to conserve the general fold of the protein. The constrained distances were kept between all αC atoms of the ligands and selected αC atoms of HCC. The constrained distances were from 3.9 to 4.8 Å, and all the force constants were kept to f = 100 kcal/(mol×Å). The typical box size was about 90×90×90 Å. The systems were diluted in TIP3P water. After minimization the MD for all systems were calculated. Simulations of the complexes in solution were performed under periodic boundary conditions in a closed, isothermal, isobaric (NTP) ensemble. Throughout the simulation the solute and solvent were coupled to a constant-temperature (T = 308 K) heat bath and a constant-pressure (P = 1 atm) bath. All hydrogen-containing bonds were constrained using the SHAKE algorithm allowing a time step of 0.0005 ps. An Ewald summation (Essman *et al.*, 1995) was used for non-bonded interactions. Coordinates were saved every 1000 steps. The time length during all MD was about 1500 ps. The time length of MD was about 300 ps with constraints and about 1200 ps without constraints. When the protein–ligand complexes started to dissociate, the MD calculations were interrupted. A detailed analysis of the obtained results was made with the use of the AMBER package programs and graphical programs like RasMol (v2.6) and MolMol (Koradi *et al.*, 1996).

Table 1. The general protocol of MD calculations; step 1 — in SYBYL program; steps 2–6 in AMBER program.

Step	Procedures
1	Building the starting complex of HCC-ligand
2	Minimization *in vacuo*
3	Adding counterions (Na^+ and Cl^-) and water molecules
4	Minimization (optimization) in water
5	Equilibration by molecular dynamics
6	Molecular dynamics productive run

RESULTS AND DISCUSSION

We have chosen the following regions of HCC which are likely to be involved in the disruption of monomeric fold required for dimer formation: $\beta 2_{42-54}$, $\beta 3_{60-73}$, $L1_{55-58}$, $L2_{105-108}$, and N-terminus$_{8-11}$. According to the proposed 3D swapping mechanism (Jaskólski, 2001), HCC dimerization starts

from an opening movement of loop L1 and separation of the β-sheet strands β2 and β3. On the other hand, the N-terminus and loops L1 and L2 contribute to the inhibition of papain-like cystein proteases (Grzonka *et al.*, 2001). This function completely disappears in HCC dimer, therefore it is possible that conformational changes within the L1, L2 and N-terminus regions may also stimulate dimerization. Figure 1 illustrates mutual hydropathic complementarity between the chosen segments and the complementary peptide chains. We expected that antisense peptides of the regions crucial for dimer formation could bind specifically with monomeric HCC and prevent its partial unfolding required for dimerization. Therefore, based on the sense mRNA sequences of the chosen regions of HCC corresponding antisense mRNA sequences were obtained and the sequences of the encoded complementary peptides were deduced (**1**, **2**, **3**, **4**, **5**, **6**, **7**, **8**, **9** (Table 2)). A combined antisense peptide of three HCC fragments (N-terminus$_{8\text{-}11}$, L1$_{55\text{-}56}$ and L2$_{107}$) that interact with cysteine proteases catalytic cleft (substrate sequence (Stacho-

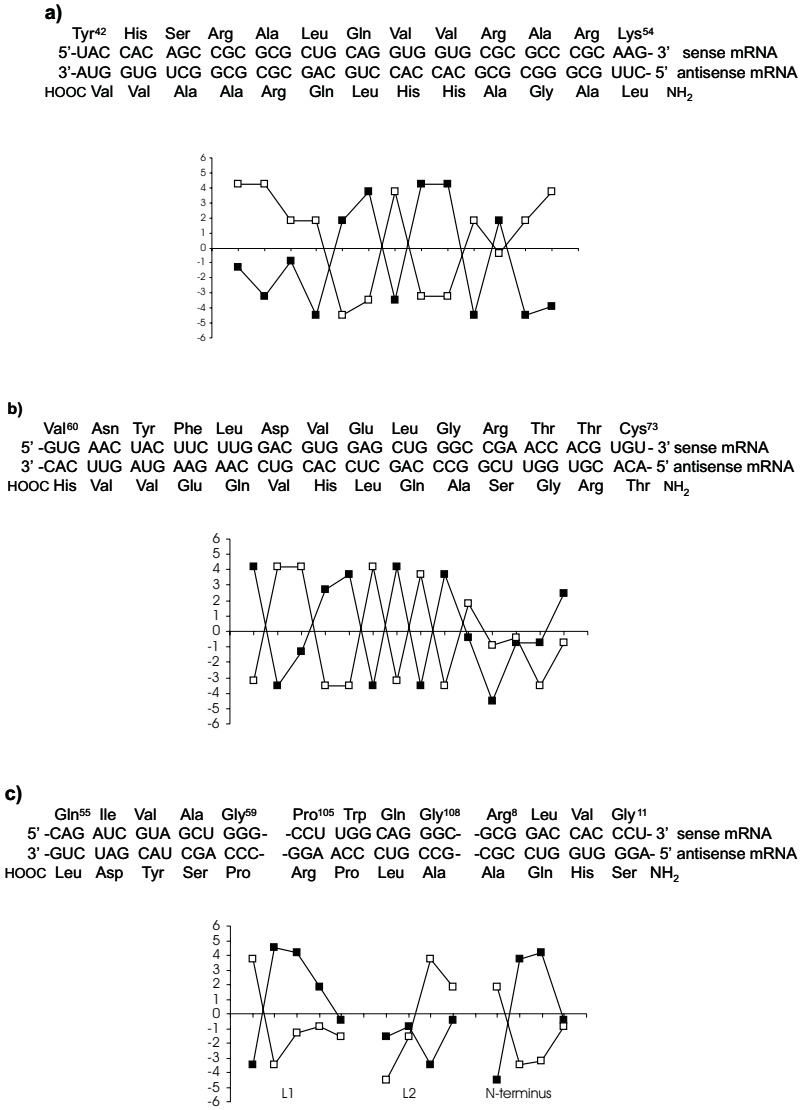

Figure 1. Antisense peptides for the following HCC fragments: a, β2$_{47-54}$; b, β3$_{60-73}$; and c, L1$_{55-58}$, L2$_{105-108}$ and N-terminus$_{8-11}$.

Hydropathic complementarity between sense (■) and antisense (❑) peptides is also shown according to the Kyte-Doolittle hydropathy scale.

wiak *et al.*, 2004)) during its inhibition was also designed (**11**). We surmised that a ligand of substrate sequence, similarly like the ligand to combined fragments of both loops (**10**) could interact simultaneously with different parts of active monomeric HCC, stabilizing it. The binding of our ligands with HCC would not interfere with its native function (as a cysteine protease inhibitor) because both interactions are reversible and the affinity of sense and antisense peptides seems to be far weaker comparing with the affinity of cysteine proteases for HCC (tight-binding inhibitor). The designed peptides were synthesized and used to study their influence on HCC dimer formation. Table 2 shows that neither of our antisense peptides was able to prevent the HCC dimerization. All the designed peptides appear to promote this process at both the 1:1 and 1:10 concentration ratio of HCC to the ligand. In the case of compounds **1**, **2**, **4** and **7** an increase of ligand concentration does not influence the dimerization level whereas the higher concentration of peptides **9** and **10** seems to decrease the amount of HCC dimer. The higher concentration of peptides **3**, **5**, **6** and **11**, in contrast, promoted the dimerization.

Table 2. Sequences of the designed antisense peptides and the progress of HCC dimerization

ID	Target fragment of HCC	Amino acid sequence of the antisense peptide	% of HCC dimer*	
			1:1	1:10
1	N-terminus$^{8-11}$	SHQA	61	64
2	N-terminus$^{8-11}$+β1$^{12-13}$	GASHQA	64	65
3	N-terminus$^{8-11}$+β1$^{12-15}$	VHGASHQA	59	67
4	N-terminus$^{8-11}$+β1$^{12-18}$	HAGVHGASHQA	75	75
5	β3$^{60-73}$	TRGSAQLHVQEVVH	70	83
6	β2$^{42-54}$	LAGAHHLQRAVV	58	74
7	β2$^{49-54}$+L1$^{55-59}$	PSYDLLAGAHH	61	61
8	L1$^{55-59}$	PSYDL	63	68
9	L2$^{105-108}$	ALPR	75	70
10	L1$^{55-58}$+L2$^{106-108}$	ALPSYDL	69	59
11	N-terminus$^{8-11}$+L1$^{55-56}$+L2^{107}	PSYSHQA	60	70

*Cystatin C was incubated with antisense peptides at a molar ratio of 1:1 and 1:10 for 7 days at 37°C and pH = 8.6. In this condition HCC without ligands shows 45% of dimer.

Additionally, we built theoretical complexes of HCC with designed ligands: the 'open' HCC form with ligands **4** and **5**; the 'closed' HCC model with ligands **6** and **8**; both 'open' and 'closed' HCC with ligand **9**. We determined the stability of the complexes (HCC–ligand) using MD simulations. According to MD studies three ligands (**4**, **5** and **6**) reveal affinity for HCC (Fig. 2a). The interactions have mainly hydrophobic (≈70%) and electrostatic character. Additionally, ligands **4** and **5** bind to the HCC protein by hydrogen bonds. The N-terminal fragment of ligand **4** moved to the β2 strand after MD calculations and created

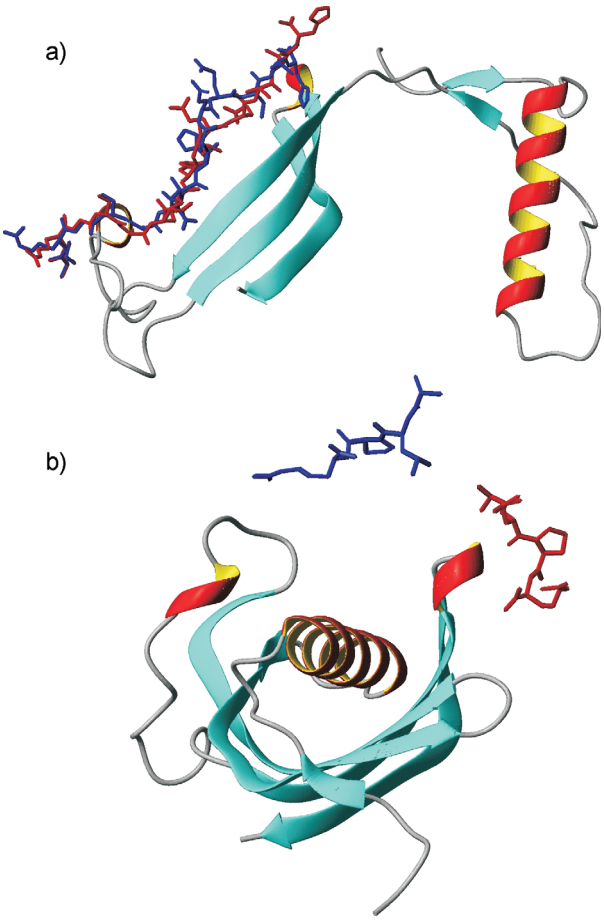

Figure 2. Structures of HCC (ribbon representation) in complex with ligands (wire frame representation), a) ligand 5 with the open form of HCC, b) ligand 9 with the closed form of HCC.

The starting structures and the structures after MD simulations were superimpose by αC atoms of HCC. The ligands are coloured red (before MD) and blue (after MD).

two hydrogen bonds between residues: R^{51} (HCC) and G^{3} (ligand) (O.... N), R^{53} (HCC) and G^{3} (ligand) (N.... O). Ligand **5** interacts by four hydrogen bonds between: E^{67} (HCC) and L^{7} (ligand) (N.... O), E^{67} (HCC) and L^{7} (ligand) (O.... N), F^{85} (HCC) and G^{3} (ligand) (N.... O), N^{82} (HCC) and R^{2} (ligand) (O.... N). Peptides **8** and **9** dissociated from the complex during the MD simulations (Fig. 2b). Water molecules entered the space between the ligands and HCC. Our MD investigations suggest that peptides **4**, **5**, and **6** interact specifically with HCC. However, these interactions probably untighten the monomeric structure of HCC and stabilize its open form facilitating the dimerization process. Several 3D domain swapping processes are known to be induced by receptor/ligand binding. 3D domain swapping regulated by ligands was reported in glyoxalase I (Saint-Jean *et al.*, 1998) and p13suc1 (Schymkowitz *et al.*, 2001), where the equilibrium between the monomer and dimer is regulated by gluthatione and phosphopeptide, respectively, suggesting that ligand binding may regulate the functions of its receptor through 3D domain swapping. Similarly, 3D domain swapping was proposed as a mechanism for the oligomerization of membrane-associated guanylate kinases regulated by their ligand binding (McGee *et al.*, 2001).

All calculations were performed on a UNIX cluster of computers in the TASK Centre and in the Molecular Modelling Group of the Faculty of Chemistry in Gdańsk.

REFERENCES

Abrahamson M. (1996) *Scand J Clin Lab Invest.*; **56**: 47–56.

Abrahamson M, Dalbege H, Olafsson I, Carlsen S, Grubb A. (1988) *FEBS Lett.*; **236**: 14–8.

Baranyi L, Campbell W, Ohshima K, Fujimoto S, Boros M, Okada H. (1995) *Nat Med.*; **1**: 894–901.

Blalock JE. (1990) *Trends Biotechnol.*; **8**: 140–4.

Blalock JE. (1995) *Nat Med.*; **1**: 876–8.

Blalock JE. (1999) *Cell Mol Life Sci.*; **55**: 513–8.

Bode W, Engh R, Musil D, Thiele U, Huber R, Karshikov A, Brzin J, Kos J, Turk V. (1988) *EMBO J.*; **7**: 2593–9.

Case DA, Pearlman DA, Caldwell JW, Cheatham III TE, Ross WS, Simmerling D, Darden T, Merz KM, Stanton RV, Cheng A, Vincent JJ, Crowley M, Ferguson DM, Radmer R, Seibel GL, Singh UC, Wiener P, Kollman PA. (1997) *Amber 5.0*. University of California, San Fransisco

Dieckmann T, Mitschang L, Hofmann M, Kos J, Turk V, Auerswald EA, Jaenicke R, Oschkinat H. (1993) *J Mol Biol.*; **234**: 1048–59.

Ekiel I, Abrahamson M. (1996) *J Biol Chem.*; **271**: 1314–21.

Ekiel I, Abrahamson M, Fulton DB, Lindahl P, Storer AC, Levadoux W, Lafrance M, Labelle S, Pomerleau Y, Groleau D, LeSauter L, Gehring K. (1997) *J Mol Biol.*; **271**: 266–77.

Engh RA, Dieckmann T, Bode W, Auerswald EA, Turk V, Huber R, Oschkinat H. (1993) *J Mol Biol.*; **234**: 1060–9.

Essman U, Perera L, Berkowitz ML, Darden TA, Lee H, Pedersen L. (1995) *J Chem Phys.*; **103**: 8577–93.

Gerhatz B, Ekiel I, Abrahamson M. (1998) *Biochemistry.*; **37**: 17309–17.

Ghiso J, Jensson O, Frangione B. (1986) *Proc Natl Acad Sci U S A.*; **83**: 2974–8.

Ghiso J, Saball E, Leoni J, Rostagno A, Frangione B. (1990) *Proc Natl Acad Sci U S A.*; **87**: 1288–91.

Grubb AO. (2000) *Adv Clin Chem.*; **35**: 63–99.

Grzonka Z, Jankowska E, Kasprzykowski F, Kasprzykowska R, Łankiewicz L, Wiczk W, Wieczerzak E, Ciarkowski J, Drabik P, Janowski R, Kozak M, JaskÓlski M, Grubb AO. (2001) *Acta Biochim Polon.*; **48**: 1–20.

Heal JR, Bino S, Ray KP, Christie G, Miller AD, Raynes JG. (1999) *Mol Immunol.*; **36**: 1141–8.

Heal JR, Bino S, Roberts GW, Raynes JG, Miller AD. (2002) *Chembiochem.*; **3**: 76–85.

Janowski R, Kozak M, Jankowska E, Grzonka Z, Grubb AO, Abrahamson M, Jaskólski M. (2001) *Nat Struct Biol.*; **8**: 316–20.

Jaskólski M. (2001) *Acta Biochim Polon.* **48**: 807–27.

Jensson O, Gudmundsson G, Arnason A, Blondal H, Petursdottir I, Thorsteinsson L, Grubb AO, Lofberg H, Cohen D, Frangione B. (1987) *Acta Neurol Scan.*; **76**: 102–14.

Jeppsson JO, Laurel CB, Franzen B. (1979) *Clin Chem.*; **25**: 629–38.

Jerela R, Zerovnik E. (1999) *J Mol Biol.*; **291**: 1079–89.

Koradi R, Billeter M, WÜtrich K. (1996) *J Mol Graphics.*; **14**: 51–5, 29–32.

Kyte J, Doolittle RF. (1982) *J Mol Biol.*; **157**: 105–32.

Martin JR, Craven CJ, Jerala R, Kroon-Zitko L, Zerovnik E, Turk V, Waltho JP. (1995) *J Mol Biol.*; **246**: 331–43.

McGee AW, Dakoji SR, Olsen O, Bredt DS, Lim WA, Prehoda KE. (2001) *Mol Cell.*; **8**: 1291–301.

Mekler LB. (1969) *Biofizika.*; **14**: 581–4.

Olafsson I, Grubb AO. (2000) *Amyloid.*; **7**: 70–9.

Saint-Jean AP, Phillips KR, Creighton DJ, Stone MJ. (1998) *Biochemistry.*; **37**: 10345–53.

Sautebin L, Rombola L, Di Rosa M, Caliendo G, Perissutti E, Grieco P, Severino B, Santagada V. (2000) *Eur J Med Chem.*; **35**: 727–32.

Schymkowitz JW, Rousseau F, Wilkinson HR, Friedler A, Itzhaki LS. (2001) *Nat Struct Biol.*; **8**: 888–92.

Staniforth RA, Giannini S, Higgins LD, Conroy MJ, Hounslow AM, Jerala R, Craven CJ, Waltho JP. (2001) *EMBO J.*; **20**: 4774–81.

Stachowiak K, Tokmina M, Karpi□ska A, Sosnowska R, Wiczk W. (2004) *Acta Biochim Polon.*; **51**: (in press).

Stubbs MT, Laber B, Bode W, Huber R, Jerala R, Lenarcic B, Turk V. (1990) *EMBO J.*; **9**: 1939–47.

SYBYL ver. 6.6 © 2000 Tripos, Inc.

Zhao R, Yu X, Liu H, Zhai L, Xiong S, Su T, Liu S. (2001) *J Chrom A.*; **913**: 421–28.